Proc. 5th Int. Workshop New Photon-Detectors (PD18)
JPS Conf. Proc. **27**, 011010 (2019)
https://doi.org/10.7566/JPSCP.27.011010

Results of the Parallel Operation of Large-size SiPM Detector Modules and PMTs in IACTs

Alexander Hahn[1,2], Antonios Dettlaff[1], David Fink[1], Daniel Mazin[1,3], Razmik Mirzoyan[1] and Masahiro Teshima[1,3]

[1]*Max Planck Institute for Physics, Föhringer Ring 6, 80805 Munich, Germany*
[2]*Physics Department, Technical University Munich, James-Franck-Str. 1, 85748 Garching, Germany*
[3]*Institute for Cosmic Ray Research, University of Tokyo Kashiwa-no-ha 5-1-5, Kashiwa-shi, 277-8582 Chiba, Japan*

E-mail: ahahn@mpp.mpg.de

(Received March 04, 2019)

We developed three prototype detector modules using silicon photomultipliers (SiPMs) instead of conventional photomultiplier tubes (PMTs) at the Max Planck Institute for Physics. These prototypes are being used to compare the performance of SiPMs and PMTs during operation in the imaging cameras of the Major Atmospheric Gamma Imaging Cherenkov (MAGIC) telescopes. The detector modules use either Hamamatsu, SensL or Excelitas devices. To achieve an active area comparable to a 1 inch PMT, we used a matrix of up to nine $6 \times 6\,\mathrm{mm}^2$ SiPMs, actively summing the individual signals while maintaining their fast signal response. The installation of the three prototype modules was completed in 2017. Since then they have been operated alongside the PMT based camera on nightly basis. The resulting data, comprised of Cherenkov light generated in extensive air showers (EAS) and artificial light pulses, is collected during telescope operation and used for performance comparisons.
The MAGIC camera structure is suitable for the installation of up to six prototype detector modules next to the PMTsfor parallel operation.
The outer camera rim, where we installed the SiPM based detector modules, is not included in the trigger. In order to gather data on operation in the trigger area one prototype module was installed to the camera centre for a single night in 2018.
The two MAGIC telescopes utilized in this study are located on the Canary Island of La Palma. Each telescope consists of a 17 m diameter mirror dish and a camera composed of 1039 PMTs.

KEYWORDS: SiPM, PMT, LLL, Multi-pixel avalanche photodiodes, IACT

1. Introduction

MAGIC is a stereoscopic system of two imaging atmospheric Cherenkov telescopes (IACTs) dedicated to observations of high energy gamma-rays. The telescopes are located at the Observatorio del Roque de los Muchachos (2200 m a.s.l.) on the Canary Island of La Palma. Both imaging cameras rely on 1039 PMTs as low light level (LLL) detectors [1, 2]. Seven of these PMT pixels are contained in each module for to a total of 169 modules per camera. The circular PMT camera leaves open 6 slots at the vertices of the hexagonal camera structure. This allows us to install 6 additional detector modules of 7 pixels each next to the working scientific instrument. Since there is no impact on the telescope performance, long term studies under real operation conditions can be performed.
Recent generations of SiPMs are competitive with PMTs in terms of peak photon detec-

tion efficiency (PDE) and in some cases exceed the PDE of PMTs.; see for example [3, 4]. Additional advantages of SiPMs as semiconductor based light sensors are the lack of ageing even at high light levels and operation without high voltages. This allows for their operation during moon time similar to the MAGIC PMT cameras [5]. The main drawbacks for the operation of SiPMs in IACTs are their temperature dependency and their high sensitivity to light of the night sky (LoNS) at long wavelengths.
We developed three new light detector modules based on matrices of silicon photomultipliers of our own design. The aim was to achieve the same size of active area per pixel as the 1 inch PMTs used by MAGIC while maintaining fast signal response and good single photo-electron separation [6]. A first prototype, based on Excelitas SiPMs, was installed to the MAGIC-1 camera in 2015 [7]. The experience gained with this first prototype was applied to the design of two second generation SiPM based modules. Hamamatsu and SensL SiPMs were used as the optical sensors in these modules. The second generation modules were installed in May 2017. All three modules are operated alongside the PMTs during data taking on a nightly basis.

2. SiPM Module Design

We combined several SiPMs per pixel to achieve the same active area as a 1 inch PMT. For the first SiPM module, we configured pixels with an array of seven $6 \times 6\,\mathrm{mm}^2$ SiPMs. One of these pixels is shown in Figure 1. For the second generation of SiPM modules, we increased the number of summed SiPMs from 7 to 9 (see Figure 1). This reduces the dead area of the pixels. The new SiPM modules have a higher sensitivity due to the higher PDE of more recent sensors.
All 7 pixels of a module are supplied with a common bias voltage. The SiPMs of each pixel are divided into three groups. By applying an offset voltage we can control the bias voltage of each of the groups individually.
Because of the temperature dependency of silicon sensors a stable operation temperature is desired. Aluminium core printed circuit boards (PCBs) were used for the second generation of SiPM pixels, reducing the thermal resistance between the sensors and the PCB core. This aluminium core is thermally coupled to the module's metal structure which is in direct contact to two cooling plates further back, reducing the temperature gradient between the sensors and the camera cooling. Due to this, the temperature variations at the sensor are significantly reduced. The individual signals of the seven SiPMs are summed by an analog transimpedance summing stage which is realized on the back side of each pixel. In this way we avoid degradation of the fast signal response which would occur by connecting the output of all SiPMs to a common point, thereby summing the sensor capacitances.

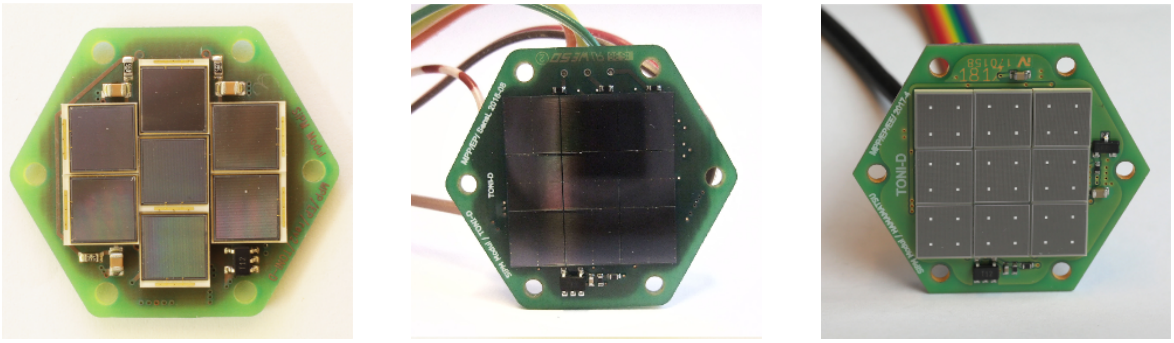

Fig. 1. A first generation SiPM pixel based on Excelitas SiPMs (left). Two second generation SiPM pixels, one based on SensL SiPMs (centre) the other based on Hamamatsu SiPMs (right).

3. Operating Characteristics for SiPMs in Atmospheric Cherenkov Telescopes

In contrast to many particle physics experiments, IACTs are not be operated at cryogenic temperatures and are exposed to the LoNS. The LoNS spectrum differs from the Cherenkov spectrum of EAS. For a high signal to noise ratio, the spectral response of the photo sensors of an IACT should closely match the Cherenkov spectrum. In Figure 2 the comparison of the PMT and SiPM photon-detection efficiencies with the LoNS and the Cherenkov spectrum is shown. It is easy to see that the SiPMs detect much more LoNS that the PMTs. This leads to additional design requirements to address the high background count rate i.e. high signal currents and the resulting sensor heating. Two other variable sources of optical background must be considered as part of the design. One is the moon light which depends on its phase and the relative pointing position of the telescope. The other source of background light is stars in the field of view of the telescope. A circuit which allows us to switch off individual pixels or even parts of the pixels to limit the currents due to stars was implemented.

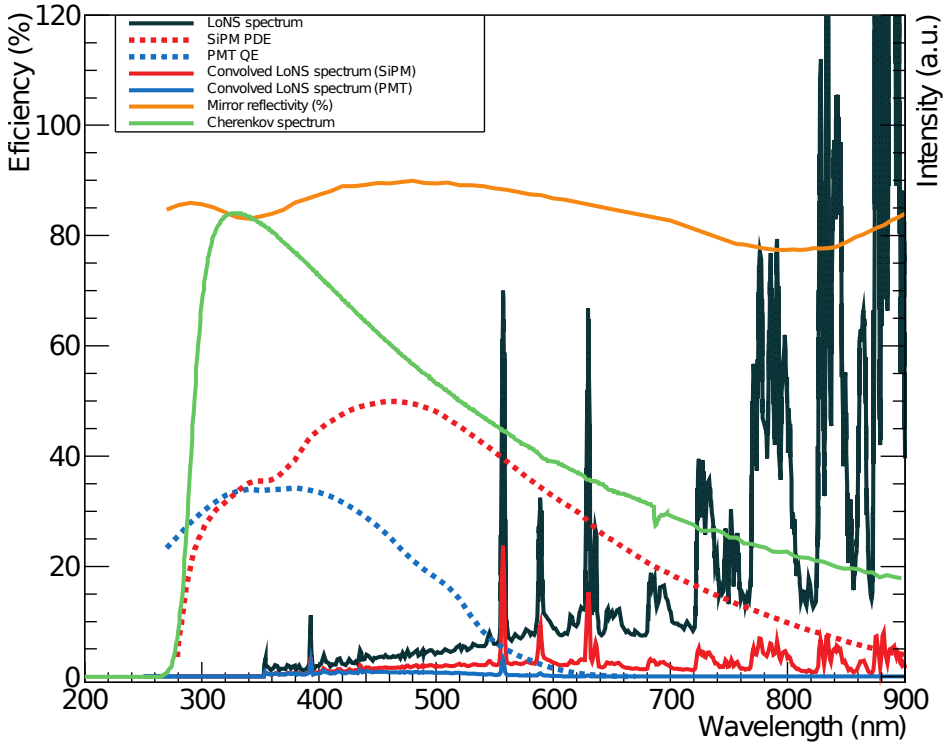

Fig. 2. Cherenkov (green) and LoNS spectrum (black), overlaid by Hamamatsu LCT5 SiPM PDE (red dashed) and Hamamatsu PMT R10408 QE curve (blue dashed) [8–10]. The multiplication of the SiPM PDE and the LoNS spectrum is shown in red and the multiplication of PMT QE and LoNS spectrum in blue. In addition the reflectivity curve of the MAGIC-1 mirror is plotted in orange.

4. Measurements and Performed Tests

We measured linearity, cross-talk, and single photo-electron response in our laboratory prior to installing the modules in the camera. The camera data taken is in good agreement with those measurements. For the calibration we investigated the use of the single photo-electron spectrum of dark counts and the so-called F-Factor (excess noise factor)

method [11, 12].
Using Figure 2, it is easy to calculate the expected performance with reference to the Hamamatsu PMTs of type R10408 used in MAGIC. The detection efficiencies of each detector type have to be multiplied with the LoNS spectrum to estimate the noise and multiplied with the Cherenkov spectrum to estimate the signal. By comparing the integrals of the multiplied spectra we calculate that the Hamamatsu SiPM pixel will detect 1.9 times more Cherenkov photons and 9.6 times more LoNS photons than the PMTs in use. Both increases are due to the higher peak sensitivity of SiPMs and the extended sensitivity to long wavelength photons. The fluctuation, which is the square root of the detected LoNS photons, thus increases the expected noise level for SiPMs by a factor of ~ 3. Here it should be noted that the numbers calculated above are valid for a direct comparison of sensors inside the MAGIC camera. Modern PMTs like the Hamamtsu R12992-100 used in the large-size telescope (LST) of the Cherenkov Telescope Array (CTA) have a significantly larger QE (43% peak QE) compared to the PMTs used in MAGIC (34% peak QE) which would lead to different numbers but a similar conclusion [13].
A light flasher is mounted at the centre of each telescope mirror dish. It flashes the entire camera with homogeneous 355 nm light flashes at a fixed repetition frequency of 25 Hz. The first performance comparison utilizes these light flashes which are used for the PMT calibration of MAGIC. Because the light is monochromatic, it is easy to compare the results with the predictions derived from the spectra shown in Figure 2.
In Figure 3, one can see the number of photo-electrons detected by representative SiPM pixels based on Hamamatsu devices and the average number of photo-electrons detected by the 1039 PMT pixels. The gains of these second generation SiPM pixels have been calibrated with the the method based on the dark count spectrum of the devices. For the shown SiPM pixels, the number of photo-electrons has been corrected for the additional contribution from cross-talk events so that only the number of detected incoming photons is shown. Taking the photon detection efficiency (PDE) at 355 nm and the dead area of the SiPM pixel into account one expects to measure around the same signal with a Hamamatsu SiPM pixel as with a PMT based MAGIC pixel. The measurement is in good agreement with that calculated prediction although there is a spread within the SiPM pixels. This spread is caused by differences in the cross-talk probability and therefore in the correction factor when subtracting the cross-talk contribution from the measured number of photo-electrons. This effect is currently under investigation.
Figure 4 also shows the number of detected photo-electrons but in contrast to the Hamamatsu SiPM pixels the SensL SiPM pixels have been calibrated with the F-Factor method. The calibration gives a reliable result which is in good agreement with the expected performance in this case as well.
Of course a fair comparison has to be based on real Cherenkov light from EASs. Because the SiPM modules are located the camera rim but the camera is triggered only on an inner region of pixels; one introduces a bias on the Cherenkov light distribution when analysing typical EAS shaped events. In order to compare the detection efficiency of the SiPMs and neighbouring PMTs one has to take the EAS morphology into account. One could select only very large events which are very wide and are more homogeneous inside the camera. Such large hadronic events have a very low count rate thus requiring the combination of a lot of data. To overcome this problem we installed the Hamamatsu SiPM module into the camera centre for one night. In this way the SiPM module can trigger the readout itself and is surrounded by a symmetric circle of PMTs thereby reducing the possible systematic uncertainties.
By comparing the individual pixel trigger rates one can check the predicted increase of the background rate caused by the higher sensitivity to LoNS photons. The pixel trigger rates

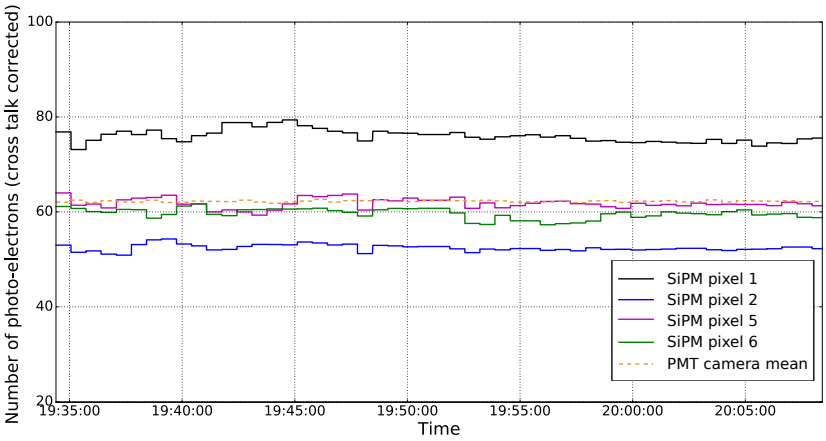

Fig. 3. Number of detected photo-electrons by second generation Hamamatsu SiPM pixels and the average of the PMTs of the camera. The gains of the SiPM pixels were calibrated using the dark count single photo-electron spectrum and have been corrected for the additional cross-talk contribution.

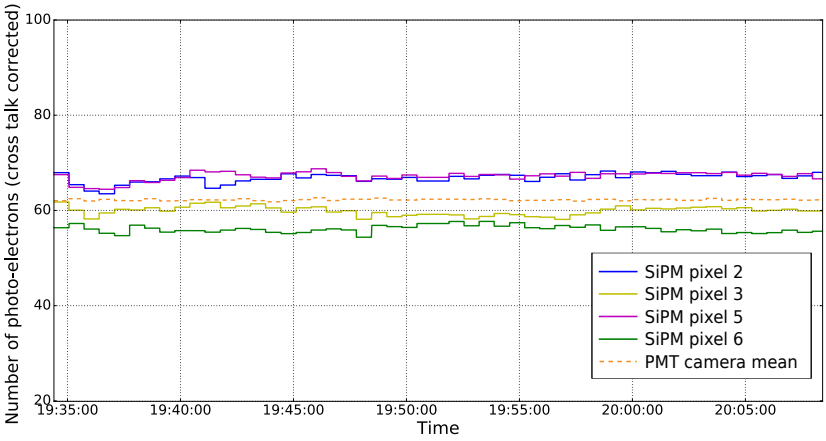

Fig. 4. Number of detected photo-electrons by second generation SensL SiPM pixels and the average of the PMTs. The gains of the SiPM pixels have been calibrated using the F-Factor method and have been corrected for the additional cross-talk contribution.

are shown in Figure 5. The trigger threshold for both detector types was set to three photo-electrons. The calculated increase by a factor of 3 is in agreement with our measurement.

5. Summary

We developed three different SiPM based detector modules for an ongoing performance evaluation study in the MAGIC camera. We demonstrated two different working calibration procedures. The temperature stability was improved with the use of aluminium core PCBs. The measured performance using artificial light flashes as well as Cherenkov light from EAS are in good agreement with the calculated expectations. SiPMs have the drawback of their small physical size but this was overcome by assembling a matrix of up to 9 SiPMs. The high PDE of SiPMs increases the number of detected photons from an EAS. This could be further improved by moving the SiPM peak PDE towards shorter wavelength. The main disadvantage of SiPMs remains their high background rate induced by LoNS photons. In a

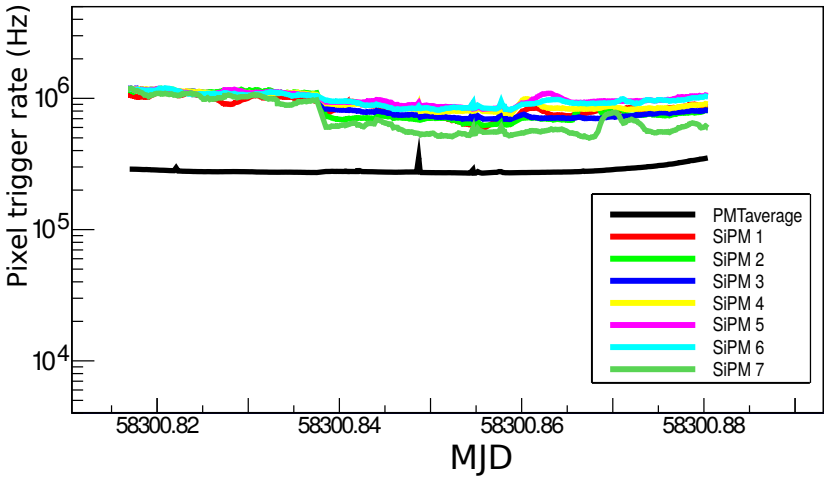

Fig. 5. Individual pixel trigger rate for all seven Hamamatsu SiPM pixels compared to the PMT camera average. The trigger threshold is set to three photo-electrons for both types of detectors.

next step, we intend to calculated the signal to noise ratio for Cherenkov light from EAS of different intensities and perform a rate scan to estimate the energy threshold of a complete SiPM based camera. The use of UV-pass filters similar to [5] might improve the signal to noise ratio further. Based on these results we consider SiPMs a good potential candidate light detector for IACTs but further study is needed.

References

[1] J. Aleksić, et al. The major upgrade of the MAGIC telescopes, Part I: The hardware improvements and the commissioning of the system, Astroparticle Physics **72**, 61 (2016)
[2] J. Aleksić, et al. The major upgrade of the MAGIC telescopes, Part II: A performance study using observations of the Crab Nebula, Astroparticle Physics **72**, 76 (2016)
[3] R. Mirzoyan, et al. Evaluation of novel PMTs of worldwide best parameters for the CTA project, NIM-A **845**, 603 (2017)
[4] A. Otte, et al. Characterization of three high efficiency and blue sensitive silicon photomultipliers, NIM-A **846**, 106 (2017)
[5] M. Ahnen, et al. Performance of the MAGIC telescopes under moonlight, Astroparticle Physics **94**, 29 (2017)
[6] D. Fink, et al. SiPM Based Focal Plane Instrumentation Prototype for the MAGIC Telescopes, Proc. of International Conference on New Photo-detectors (2015)
[7] A. Hahn, et al. Development of a composite large-size SiPM (assembled matrix) based modular detector cluster for MAGIC, NIM-A **845**, 89 (2017)
[8] M. Doering, et al. Measurement of the Cherenkov light spectrum and of the polarization with the HEGRA-IACT-system, Proc. of 27th International Cosmic Ray Conference (2001)
[9] C. Benn, et al. LA Palma Night-Sky Brightness, New Astronomy Reviews **42**, 503 (1998)
[10] D. Nakajima, et al. New Imaging Camera for the MAGIC-I Telescope, Proc. of 33rd International Cosmic Ray Conference (2013)
[11] A. Hahn, et al. Development of three silicon photomultiplier detector modules for the MAGIC telescopes for a performance comparison to PMTs, NIM-A **912**, 259 (2018)
[12] R. Mirzoyan, et al. On the Calibration Accuracy of Light Sensors in Atmospheric Cherenkov, Fluorescence and Neutrino Experiments, Proc. of 25th International Cosmic Ray Conference **7**, 265 (1997)
[13] T. Toyama, et al. Evaluation of the basic propertied of the novel 1.5 in. size PMTs from Hamamatsu Photonics and Electron Tubes Enterprises, NIM-A **787**, 280(2015)